Polish Society of Composite Materials
Polskie Towarzystwo Materiałów Kompozytowych

20: 1 (2020) 35-42

COMPOSITES THEORY AND PRACTICE
ISSN: 2084-6096
ISSN (online): 2299-128X

Marian Klasztorny[1a]*, Daniel B. Nycz[2], Pawel Bogusz[1]

[1] *Military University of Technology, ul. gen. S. Kaliskiego 2, PL-00908 Warsaw, Poland*
[2] *Jan Grodek State University in Sanok, ul. A. Mickiewicza 21, PL-38500 Sanok, Poland*
[a] *At present: Professor Emeritus in Civil and Mechanical Engineering*
**Corresponding author. E-mail: m.klasztorny@gmail.com*

Received (Otrzymano) 2.01.2020

RHEOLOGICAL EFFECTS IN IN-PLANE SHEAR TEST AND IN-PLANE SHEAR CREEP TEST ON GLASS-VINYL-ESTER LAMINA

The research concerns an E-glass/vinyl-ester composite reinforced with a balanced orthogonal stitched fabric. According to the EN ISO 14129 standard, the in-plane shear modulus and in-plane shear strength for this composite type are identified from a ±45º off-axis tension test at the crosshead displacement rate of 2 mm/min. The study presents the results of experimental quasi-static ±45º off-axis tension tests in a small shear strain range, aimed at demonstrating that the high nonlinearity of the shear stress-shear strain curve is caused by viscoelastic flow of the resin at low levels of shear stress and by viscoelastic flow and plastic micro cracks of the resin at high levels of shear stress. The tests were conducted applying four quasi-static displacement rates. It was shown that the shear stress-strain curve course and the shear strength value strongly depend on the crosshead displacement rate. To confirm the nonlinearity explanation, a classic short-term (1 hour) in-plane shear creep test was carried out on ±45º off-axis specimens subjected to in-plane shear stress equal to 67% of the average in-plane shear strength calculated according to the EN ISO 14129 standard. The ply sequence blocking viscoelastic flow and plastic micro cracks of the resin was recommended.

Keywords: fibre-reinforced polymer-matrix composite, balanced orthogonal stitched fabric, vinyl-ester resin, in-plane shear test, in-plane shear creep test, rheological effects

EFEKTY REOLOGICZNE W PRÓBIE ŚCINANIA ORAZ PEŁZANIA PRZY ŚCINANIU W PŁASZCZYŹNIE LAMINY WINYLOESTROWO-SZKLANEJ

Przedmiotem badań jest kompozyt polimerowy winyloestrowo-szklany (szkło E) wzmocniony tkaniną zszywaną ortogonalną zrównoważoną. Zgodnie z normą PN-EN ISO 14129, moduł ścinania i wytrzymałość na ścinanie w płaszczyźnie laminy tego typu kompozytu wyznacza się z próby ścinania przez rozciąganie po kątem ±45º do kierunku wątku/osnowy, przy szybkości przemieszczenia trawersy maszyny wytrzymałościowej 2 mm/min. Przedstawiono wyniki eksperymentalnej quasi-statycznej próby ścinania przez rozciąganie po kątem ±45º do kierunku wątku/osnowy ukierunkowane na wykazanie, że silna nieliniowość wykresu naprężenie styczne-odkształcenie postaciowe jest wywołana płynięciem żywicy przy małych poziomach naprężenia stycznego oraz płynięciem i mikropęknięciami żywicy przy dużych poziomach naprężenia stycznego. Próby quasi-statyczne przeprowadzono dla czterech szybkości przemieszczeń trawersy. Wykazano, że kształt wykresu naprężenie styczne-odkształcenie postaciowe oraz wartość wytrzymałości na ścinanie w płaszczyźnie laminy silnie zależą od szybkości przemieszczenia trawersy. W celu potwierdzenia wyjaśnienia nieliniowości przeprowadzono próbę pełzania krótkotrwałego (1 godzina) przy ścinaniu w płaszczyźnie laminy na próbkach rozciąganych pozaosiowo ±45º, poddanych działaniu naprężenia stycznego w płaszczyźnie laminy równego 67% średniej wytrzymałości na ścinanie w płaszczyźnie laminy według normy PN-EN ISO 14129. Rekomendowano sekwencję warstw blokującą płynięcie lepkosprężyste i mikropęknięcia żywicy.

Słowa kluczowe: kompozyt polimerowy wzmocniony włóknem, tkanina zszywana ortogonalna zrównoważona, próba ścinania w płaszczyźnie laminy, próba pełzania przy ścinaniu w płaszczyźnie laminy, efekty reologiczne

INTRODUCTION

The choice of the fibre-reinforced polymer-matrix (FRPM) composite material model for the laminae and identification of the lamina material constants are of key importance in the design calculations of FRPM composite structures. One of the commonly used structural composite materials is a stitched fabric-reinforced polymer-matrix laminate. In CAE systems, the laminae are usually modelled as a linearly elastic-brittle orthotropic/monotropic material.

In order to determine the elasticity, strength and ultimate strains constants of FRPM composites, standard and non-standard strength tests are used/proposed, carried out on specimens made of new (virgin) material, under normal conditions. To date, the following stan-

dard test methods have been developed to determine the in-plane shear properties of FRPM composites:
- rail shear method using the two- or three-rail shear test [1];
- V-notched beam method [2];
- ±45° off-axis tension test method [3, 4].

The latter test is the simplest and based on the stress–strain response of a ±45° off-axis laminate with a ply sequence symmetrical about the midplane.

A quasi-static ±45° off-axis tension test, performed in accordance with the specifications in Refs. [3, 4], leads to a well-known strongly non-linear shear stress--shear strain curve. The standard procedure is based on displacement-controlled loading at a crosshead displacement rate of 2 mm/min and defines the initial in-plane shear modulus, the ultimate in-plane shear strain (0.05) and the in-plane shear strength corresponding to the in-plane shear strain ≤ 0.05. The non-linearity of the shear stress-strain curve is neither explained nor taken into consideration in these standards.

Quasi-static ±45° off-axis tension/compression tests were investigated in Refs. [5-13] on various FRPM composite materials with thermoset or thermoplastic matrices, at different crosshead displacement ratios. Only short-term displacement-controlled processes were investigated. The following laminae were tested: woven glass/polyester [5], unidirectional carbon/epoxy [6, 11, 12], unidirectional graphite/polyimide [7], unidirectional glass/epoxy [8, 9], unidirectional carbon/polymer matrix (undefined) [10], stitched glass/vinyl-ester [13]. The following crosshead displacement ratios were used: 0.1 mm/min [6], 0.6 mm/min [10, 12], 2 mm/min [8, 11, 13], and 5 mm/min [5]. The in-plane shear using a ±45° tensile test, characterized by significant non-linearity of the shear stress-shear strain curves, was interpreted as the result of polymeric matrix plastic yielding [5-12]. Since plastics are elastic-brittle materials, plastic yielding is in the form of progressive micro cracking. The damage mechanism in plastics differs from that in metals. In the ±45° tensile tests, the effect of increasing stiffness due to fibre rotation and decreasing stiffness due to damage evolution in a large deformation range was investigated in Refs. [7, 12].

Correct physical interpretations of the in-plane shear stress-strain responses including viscoelasticity of the polymeric matrix could not be formulated because of the lack of crosshead displacement rate testing as well as the lack of creep and reverse creep tests. The viscoelastic properties of polymers and polymer-matrix composites are discussed in a large number of papers including Refs. [14-18]. In Refs. [14, 15], constitutive viscoelastic modelling of unidirectional glass/polyester composites was developed using a fractional exponential function. In Refs. [16, 17], the analytical constitutive viscoelastic modelling of thermosets was formulated.

Prediction of the creep failure time for selected polymers and polymer-matrix composite was analysed in Ref. [18]. The following materials were tested: Nylon 66 (thermoplastic), glass-fibre nylon-matrix composite, PC Lexan 141 (thermoplastic), and T300/VE (carbon-fibre vinyl-ester-matrix composite). The analysis took into account the viscoelastic path at small strains and the viscoplastic path at higher stresses. The creep failure time, defined as the time when the creep rate reaches the minimum, was determined for the above specified materials at a variety of stress levels. Creep rupture at high levels of stress is caused by viscoelastic strains, primary and secondary bond rupture, shear yielding and cracking, chain slippage, void formation and growth, as well as fibre breakdown. Temperature, stress level and time are crucial factors for the creep response of plastics and FRPM composites.

This study attempts to investigate the reasons for the high non-linearity of the in-plane shear stress-shear strain curve in a quasi-static ±45° off-axis tension test and provides recommendations on ply sequences for FRPM composite structures resulting from the tests conducted on a stitched E-glass fabric-reinforced vinyl-ester-matrix composite. Comparative analysis of the material characteristics up to failure vs. the strain ratio was performed.

MATERIAL SPECIFICATION

The experimental in-plane shear tests concern a glass fibre-reinforced plastic (GFRP) composite, designated as G/V, which is a layer of laminates made of the following components:
- matrix: Polimal VE-11M resin (producer: CIECH Sarzyna S.A., Nowa Sarzyna, Poland),
- reinforcement: GBX800 [45/–45] fabric (producer: DIPEX Co., Slovakia).

Polimal VE-11M resin (designation V) is a flame retardant neutral vinyl-ester resin with high thermal and chemical resistance. The curing system per 1 kg of this resin, at a temperature above 18°C and low air humidity, consists of Cobalt accelerator Co 1% (10 ml) and MEKP low reactive hardener (20 ml). The resin requires post curing at the increased temperature of 80°C for 4 hours. The basic parameters of this resin before and after curing/post curing are summarized in Table 1. Resin V is adapted for vacuum infusion technology [19].

Fabric GBX800 [45/–45] (designation G) is a quasi-balanced orthogonal bi-directional stitched E-glass fabric of 800 g/m^2 areal mass density. With respect to the longitudinal axis of a fabric strip and test specimens, fabric G has a [45/–45] = [±45] warp/weft orientation.

G/V composite plates with the $[2G]_S = [\pm 45]_{2S}$ fabric sequence, from which test specimens were cut, were fabricated by ROMA Co. Ltd., Grabowiec, Poland, using vacuum infusion technology. The plates were post cured according to Ref. [19]. The average values of the main parameters of a lamina are: thickness 0.663 mm, fibre volume fraction 48%, mass density 1.70 g/cm^3.

TABLE 1. **Parameters of Polimal VE-11M resin [19]**
TABELA 1. **Parametry żywicy Polimal VE-11M [19]**

Parameter, standard	Unit	Value
Viscosity at 25ºC, DIN 53015	[mPa · s]	300÷500
Gelation time at 25ºC, ISO 2535	[min]	10÷30
Tensile strength, ISO 527-2	[MPa]	80
Relative elongation at break, ISO 527-2	[%]	3.5
Tensile modulus, ISO 527-2	[MPa]	3500
Heat distortion temperature under load (HDT), ISO 75-2	[ºC]	85

MATERIAL MODEL AND IN-PLANE SHEAR TEST SPECIFICATIONS

An in-plane shear test of the G/V laminate under stretching at an angle of ±45º to the warp and weft direction was carried out on rectangular samples of dimensions $L \times b = 250 \times 25$ mm (Fig. 1). To reduce the stress concentrations at the tab ends, the 50 mm long standard tabs were lengthened by 20 mm without changing the clamping position. The sample measuring section length was therefore 110 mm. The samples were made and conditioned according to Ref. [4].

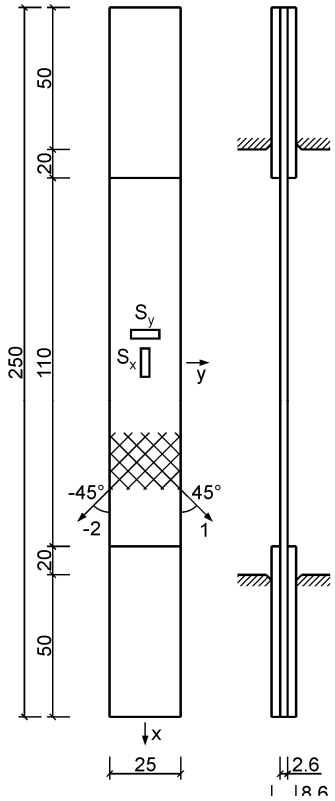

Fig. 1. Specimens used in ±45° off-axis tension test (dimensions, warp/weft orientation, strain gauges S_x, S_y, tabs, clamping)

Rys. 1. Próbki użyte w teście rozciągania pozaosiowego ±45° (wymiary, orientacja włókien wątku i osnowy, tensometry S_x, S_y, nakładki, zamocowanie)

After homogenization, composite G/V is commonly modelled as a linear elastic-brittle orthotropic material. The orthotropic axes reflect: 1 - warp direction, 2 - weft direction, 3 - thickness direction. Axes 1, 2 are at an angle of ±45º to the *x*, *y* axes, where *x* - sample axis (tension direction), *y* - in-plane transverse axis. The homogenised material is described by 9 effective elastic constants and 9 effective strength/ultimate strain constants, i.e. E_1, E_2, E_3 - Young's modules; ν_{12}, ν_{13}, ν_{23} - Poisson's ratios; G_{12}, G_{13}, G_{23} - shear modules; R_{1t}, R_{2t}, R_{3t} - tensile strengths; R_{1c}, R_{2c}, R_{3c} - compressive strengths; R_{12}, R_{13}, R_{23} - shear strengths; e_{1t}, e_{2t}, e_{3t} - ultimate normal strains under tension; e_{1c}, e_{2c}, e_{3c} - ultimate normal strains under compression; g_{12}, g_{13}, g_{23} - ultimate shear strains [20]. Composite G/V is bisymmetric, hence $E_1 = E_2$, $\nu_{13} = \nu_{23}$, $G_{13} = G_{23}$, $R_{1t} = R_{2t}$, $R_{1c} = R_{2c}$, $R_{13} = R_{23}$.

An in-plane shear test under tension at an angle of ±45º to the weft/warp direction results in a planar stress state in the 12/*xy* plane. Let us denote: $\sigma_x, \sigma_y, \tau_{xy}$ - stress state components in the *xy* system; $\varepsilon_x, \varepsilon_y, \gamma_{xy}$ - strain state components in the *xy* system; $\sigma_1, \sigma_2, \tau_{12}$ - stress state components in the 12 system; $\varepsilon_1, \varepsilon_2, \gamma_{12}$ - strain state components in the 12 system; b, h - cross section dimensions of a sample in the measurement section, P - force stretching a sample in the *x*-axis direction.

The sample meets the symmetry conditions with respect to the *x*-axis (bisymmetric orthotropic material, bisymmetric fabric sequence). Standards [1-4] assume that the sample material is homogeneous, hence force P induces a uniaxial stress state and a biaxial deformation state in the *xy* system in the measuring part of the sample, i.e.:

$$\sigma_x = P/bh, \;\; \sigma_y = 0, \;\; \tau_{xy} = 0, \\ \varepsilon_x > 0, \;\; \varepsilon_y < 0, \;\; \gamma_{xy} = 0 \qquad (1)$$

Transformation of the stress and strain states from system *xy* to system 12 (45º rotation) gives the following results, (e.g. [21]):

$$\sigma_1 = \sigma_2 = \tau_{12} = \sigma_x/2, \\ \varepsilon_1 = \varepsilon_2 = \big(\varepsilon_x + \varepsilon_y\big)/2, \;\; \gamma_{12} = \varepsilon_x - \varepsilon_y \qquad (2)$$

Formulae (2) for calculating τ_{12}, γ_{12} were introduced into the standard specifications [4], where $\varepsilon_x, \varepsilon_y$ are normal strains in the *x*, *y* directions, recorded by means of strain gauges stuck on the sample surface in its central part. In Ref. [4], a shear modulus in plane 12 was calculated from the formula based on the initial quasi-linear section of the shear stress vs. shear strain graph. The equivalent notation of this formula is as follows:

$$G_{12} = \frac{\Delta\tau_{12}(\gamma_{12})}{\Delta\gamma_{12}} = \frac{\tau_{12}(0.005) - \tau_{12}(0.001)}{0.004} \qquad (3)$$

Other specifications in Ref. [4] are as follows:

$$R_{12} = \tau_{12,\max} = \frac{P_{\max}}{2bh}, \;\; g_{12} = \gamma_{12,\max} \qquad (4)$$

where: R_{12} - in-plane shear strength, g_{12} - ultimate in-plane shear strain, $P_{\max}$ - stretching force at rupture ($g_{12} < 0.05$) or without rupture of a sample ($g_{12} = = 0.05$).

The sample material is not in a pure shear state, because there are also normal stresses σ_1, σ_2 associated with the maximum shear stress τ_{12}. The normal stresses are transferred mainly through the fibres, while the maximum shear stress is mainly transferred through the polymeric matrix. The normal stresses lead to a slight reduction in the in-plane shear strength.

TEST PLAN AND TEST PREPARATION

An in-plane shear test under tension at an angle of ±45° to the warp/weft direction is carried out on a testing machine at a constant crosshead displacement rate. The standard rate is 2 mm/min. The following hypothesis is formulated in this study. The high non-linearity of graph $\tau_{12}(\gamma_{12})$ in the in-plane shear test performed according to standard specifications [3, 4] is of the viscoelastic type at small levels of shear stress and of viscoelastic and viscoplastic types at high levels of shear stress. To prove this hypothesis, in-plane shear tests were conducted employing the following crosshead displacement rates:

1. $v_x = 0.02$ mm/min, $\dot{\varepsilon}_x = 0.000003/s$,
2. $v_x = 2$ mm/min, $\dot{\varepsilon}_x = 0.0003/s$,
3. $v_x = 20$ mm/min, $\dot{\varepsilon}_x = 0.003/s$,
4. $v_x = 2000$ mm/min, $\dot{\varepsilon}_x = 0.3/s$,

where $\dot{\varepsilon}_x$ is the normal strain ratio of the 110 mm long measuring section. For each rate the in-plane shear test (±45° off-axis tension test) was repeated on 5 samples.

Vishay 06-060LZ-120/E strain gauges (strain gauge constant 2.14) stuck in directions *x*, *y*, in the central part of the measuring section were used. The tests were performed at room temperature (20°C) and humidity ~50% using an INSTRON 8802 universal testing machine. The Traveller CF strain gauge bridge coupled to the computer was used to conduct measurements, which recorded the strain course vs. time with a sampling frequency adjusted to the crosshead displacement rate (0.5, 10, 50, 5000 Hz) and synchronized this data with the force and displacement signals recorded by the testing machine and output to the channel measuring bridge.

The in-plane shear tests were conducted in the Laboratory of Strength of Materials and Structures, Institute of Mechanics and Computational Engineering, Faculty of Mechanical Engineering, Military University of Technology, Warsaw, Poland. Selected photographic documentation of samples before and after the tests is shown in Figures 2 and 3.

The short-term in-plane shear creep test (an hour creep time) was carried out on five samples analogous to those used in the in-plane shear tests. The in-plane shear creep test was performed under 2/3 of the average in-plane shear strength determined at the standard crosshead displacement rate of 2 mm/min. It results in: $\tau_{12} = 0.667 \times R_{12} = 31.6$ MPa, $P_0 = 4.1$ kN, where P_0 is a stretching force. Force P_0 was applied at the rate of 200 kN/s. After reaching P_0 within 0.002 s, the loading force and piston displacement of the testing machine were recorded at a sampling frequency of 2 Hz.

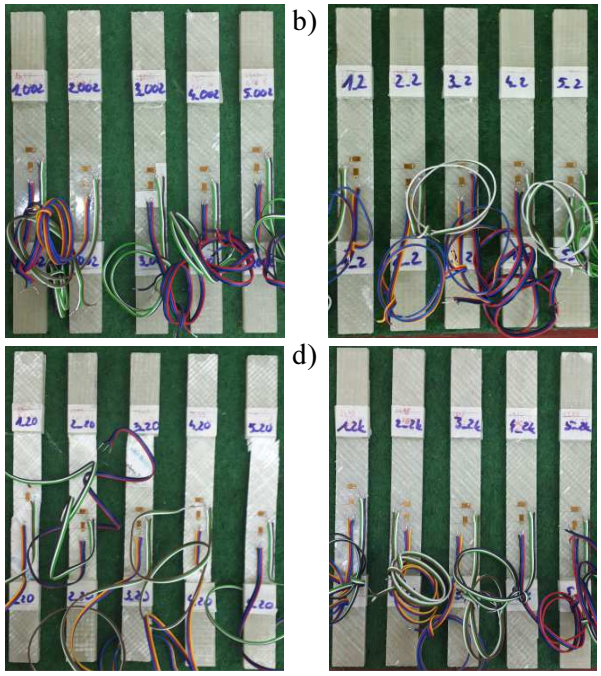

Fig. 2. Photographs of samples with stuck strain gauges, for in-plane shear tests: a) $v_x = 0.002$ mm/min (before tests); b) $v_x = 2$ mm/min (before tests); c) $v_x = 20$ mm/min (after tests); d) $v_x = 2000$ mm/min (before tests)

Rys. 2. Zdjęcia próbek z naklejonymi tensometrami do testów ścinania w płaszczyźnie laminy: a) $v_x = 0.002$ mm/min (przed testami); b) $v_x = 2$ mm/min (przed testami); c) $v_x = 20$ mm/min (po testach); d) $v_x = 2000$ mm/min (przed testami)

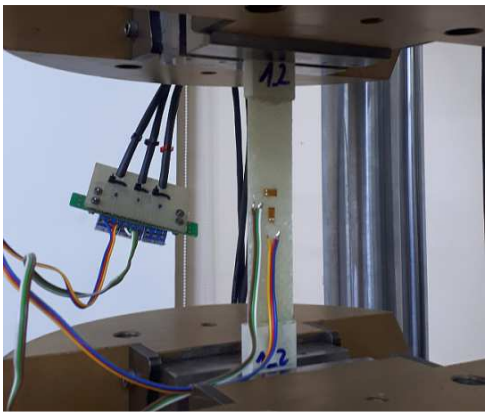

Fig. 3. Fastening exemplary specimen in Instron 8802 testing machine grips

Rys. 3. Zamocowanie przykładowej próbki w uchwytach maszyny wytrzymałościowej Instron 8802

IDENTIFICATION AND ANALYSIS OF RESULTS

The identification results describe a single homogenised lamina reinforced with fabric G. Based on the quasi-static in-plane shear tests, the in-plane shear curves $\tau_{12}(\gamma_{12})$, in-plane shear modulus G_{12}, and in-plane shear strength R_{12} were determined.

Figures 4-7 present the in-plane shear stress-shear strain curves for the adopted crosshead displacement

rates, including sample graphs (in grey) and the average path (in red). Figure 9 compares the average in-plane shear stress-shear strain curves corresponding to four crosshead rates taken into consideration. Table 2 summarizes the mean values and standard deviations for material constants G_{12}, R_{12}, derived from the graphs shown in Figures 4-7 according to Refs. [3, 4].

TABLE 2. **Mean values and standard deviations (SD) for in-plane shear modulus and in-plane shear strength of lamina G/V, derived in accordance with Refs. [3, 4]**

TABELA 2. **Wartości średnie i odchylenia standardowe (SD) modułu ścinania i wytrzymałości na ścinanie w płaszczyźnie laminy G/V, wyznaczone zgodnie z normami [3, 4]**

v_x [mm/min]	G_{12} [MPa]	SD(G_{12}) [MPa]	R_{12} [MPa]	SD(R_{12}) [MPa]
0.02	3395	74	38.4	0.6
2	3885	109	47.4	1.9
20	3952	194	49.3	1.6
2000	3502	100	58.2	3.1

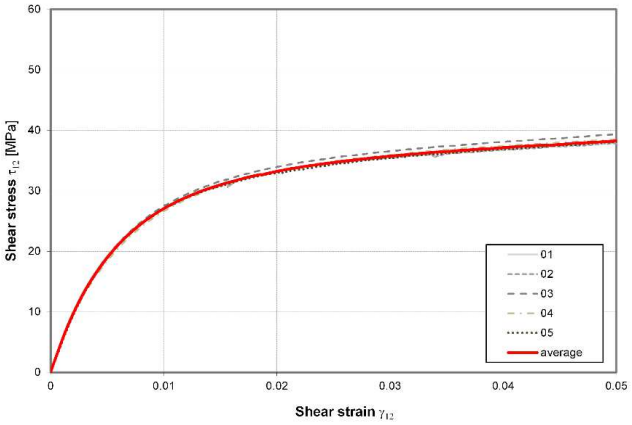

Fig. 4. In-plane shear stress-shear strain curves corresponding to crosshead rate 0.02 mm/min

Rys. 4. Krzywe naprężenie styczne-odkształcenie postaciowe w płaszczyźnie laminy, odpowiadające szybkości trawersy 0,02 mm/min

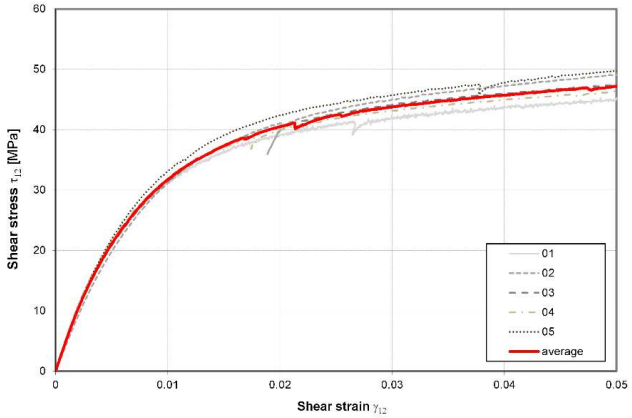

Fig. 5. In-plane shear stress-shear strain curves corresponding to crosshead rate 2 mm/min

Rys. 5. Krzywe naprężenie styczne-odkształcenie postaciowe w płaszczyźnie laminy, odpowiadające szybkości trawersy 2 mm/min

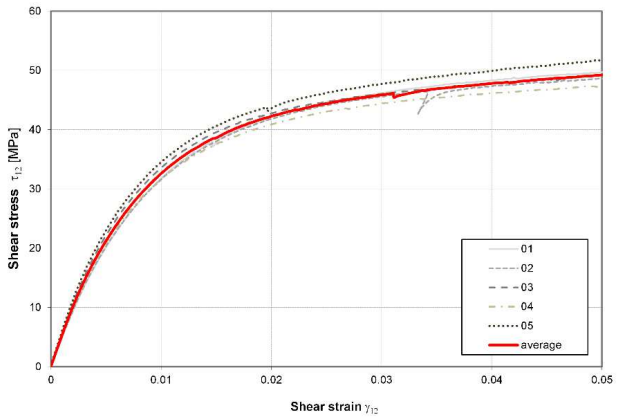

Fig. 6. In-plane shear stress-shear strain curves corresponding to crosshead rate 20 mm/min

Rys. 6. Krzywe naprężenie styczne-odkształcenie postaciowe w płaszczyźnie laminy, odpowiadające prędkości trawersy 20 mm/min

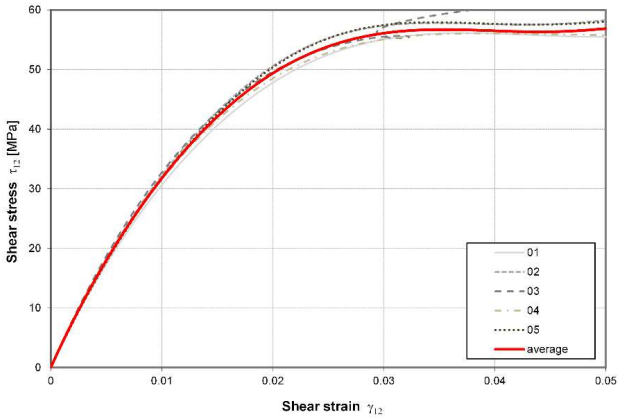

Fig. 7. In-plane shear stress-shear strain curves corresponding to crosshead rate 2000 mm/min

Rys. 7. Krzywe naprężenie styczne-odkształcenie postaciowe w płaszczyźnie laminy odpowiadające prędkości trawersy 2000 mm/min

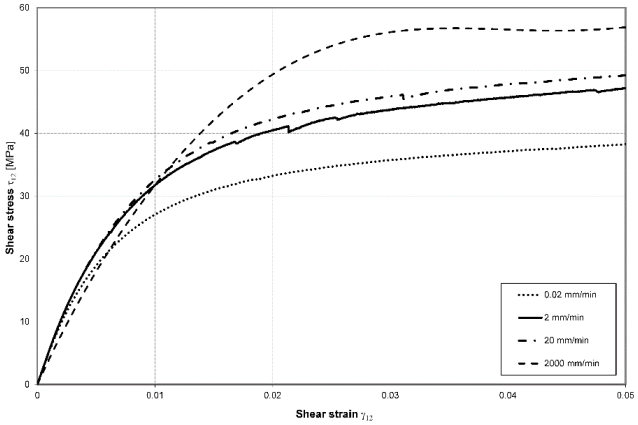

Fig. 8. Comparison of average in-plane shear stress-shear strain curves for lamina G/V

Rys. 8. Porównanie uśrednionych krzywych naprężenie styczne-odkształcenie postaciowe w płaszczyźnie laminy G/V

Based on the graphs shown in Figures 4-8, the experimental results for the in-plane shear strain $\gamma_{12} > 0.05$, and the in-plane parameter values listed in Table 2, the following conclusions were formulated:

- At a given crosshead ratio, dispersion of the shear stress–strain curves for individual samples is small, which confirms good structural repeatability of the samples.
- The average in plane shear stress-strain curve in Figure 4 confirms the viscoelastic behaviour of the composite. This is a displacement-controlled process at the low displacement ratio of 0.02 mm/min, not a classic creep process. The standard in-plane shear strength R_{12} corresponds to $\gamma_{12} = 0.05$ and is significantly underestimated. Shear strain $\gamma_{12} = 0.05$ corresponds to the longitudinal strain $\varepsilon_x = 2.3\%$, which is much smaller than the ultimate normal strain 3.5% for resin V.
- The conclusions corresponding to the average shear stress-strain curves at the medium ratio of 2 mm/min (Fig. 5) and at the high ratio of 20 mm/min (Fig. 6) are analogous to those at the low ratio of 0.02 mm/min. The stretching process lasts 100 and 1000 times shorter, respectively, hence the viscous flow of the composite is correspondingly smaller in the range $\gamma_{12} = 0 \div 0.05$. In the strain range $\gamma_{12} > 0.015$, there are irregularities confirming accumulating micro cracks of the polymer matrix. The R_{12} strength values at $\gamma_{12} = 0.05$ are correspondingly higher, but still underestimated.
- Viscous flow of the resin begins at the starting point of displacement-controlled stretching, which translates into an increase in the value of the in-plane shear modulus G_{12} as the displacement ratio increases (Figs. 4, 5, 6 and Table 2).
- The in-plane shear test at the very high displacement rate of 2000 mm/min = 33.33 mm/s is almost instantaneous; the test duration is 0.22 s (Fig. 7). The viscous flow phenomenon is negligible. The composite quickly achieves the proper shear strength R_{12} = 58.2 MPa. In the shear strain range $\gamma_{12} = [0.02; 0.05]$, there is a plastic flow phase, i.e. quickly accumulated micro cracks of the polymeric matrix. Two specimens broke at $\gamma_{12} = 0.050$, one at $\gamma_{12} = 0.072$ and two at $\gamma_{12} = 0.093$.
- Comparison of the average in-plane shear stress--strain curves for lamina G/V (Fig. 7) shows an increasing viscous flow with a reducing a crosshead displacement rate. The rates of 0.02 mm/min, 2 mm/min, and 20 mm/min are inadequate to determine the proper value of the in-plane shear strength R_{12}. The values of the in-plane shear modulus G_{12} are similar to each other for the tested ratios. At the very high quasi-static displacement ratio (v_x = 2000 mm/min), a reduction by 11% in the in-plane shear modulus is observed, compared to v_x = 20 mm/min. This phenomenon requires further investigations.
- Values R_{12}, G_{12} listed in Table 2 and their standard deviations for four quasi-static displacement rates confirm good repeatability of the results for the series of samples. The quasi-instantaneous test (v_x = 2000 mm/min) allows the actual in-plane shear strength of lamina G/V to be determined.

The short-term in-plane shear creep test, lasting an hour and corresponding to the in-plane shear test, enables the in-plane creep curve $\gamma_{12}(t), t \in [0; 60]$(min) and the in-plane shear creep modulus $G_{12}(t) = \tau_{12}/\gamma_{12}(t)$, t = 0.1 min, 1 min, 60 min to be determined. Figure 8 shows the short-term creep curves for five specimens (in grey) and the mean creep line (in red). Table 3 summarizes the average values of the in-plane shear strain and the in-plane shear creep modulus at representative time points.

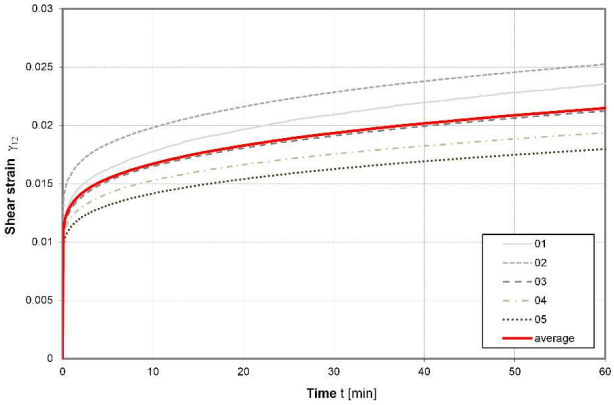

Fig. 8. Short-term creep curves corresponding to in-plane shear creep test for lamina G/V

Rys. 8. Krzywe pełzania krótkotrwałego odpowiadające testowi pełzania przy ścinaniu w płaszczyźnie laminy G/V

Figure 9 illustrates the physical model of a unit cell of lamina G/V. Before stretching, the fibres are located at angles of ±45° to the sample axis and form square sides. The interior is filled with the polymeric matrix. Normal stresses σ_1, σ_2 calculated according to Eqs. (2) cause immediate (elastic) small deformations that change the square cell into a diamond, and then in-plane shear creep of the resin starts. During creep, the fibres only rotate (glass fibres are elastic). According to Ref. [18], the in-plane shear creep process of the polymeric matrix (a semi-solid material) manifests itself in shear yielding and chain slippage.

TABLE 3. **Mean values and standard deviations (SD) of in-plane shear strain and in-plane shear creep modulus for lamina G/V at selected time points**

TABELA 3. **Wartości średnie i odchylenia standardowe (SD) odkształcenia postaciowego i modułu ścinania przy pełzaniu w płaszczyźnie laminy G/V w wybranych punktach czasowych**

Quantity	Time t [min]		
	0.1	1	60
$\gamma_{12}(t)$	0.0109	0.0132	0.0215
SD(γ_{12})	0.0014	0.0017	0.0030
$G_{12}(t)$ [MPa]	2926	2421	1494
SD(G_{12}) [MPa]	356	301	207

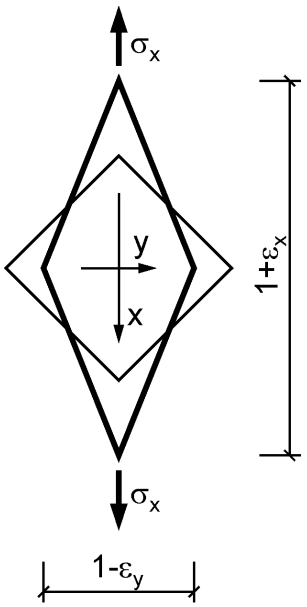

Fig. 9. Unit cell model for composite G/V in ±45° off-axis tension test

Rys. 9. Model jednostkowej celi kompozytu G/V w teście rozciągania pozaosiowego ±45°

The following conclusions are derived from the short-term in-plane shear creep test results:

- In the short-term in-plane shear creep test, corresponding to the in-plane shear test under tension at an angle of ±45° to the warp/weft direction, the polymer creep is almost unconstrained and reaches high values during the first hour of the process; the average shear strains were increased by 97%.
- The quasi-steady in-plane shear creep process begins after about 20 minutes. The creep curves for individual samples are almost identical in shape. Relatively large vertical shifts of the creep curves for individual samples result from omitting the geometrical and material imperfections of the samples when determining loading force P_0 equal for all the samples. The relatively large standard deviations of the in-plane shear creep strains and the in-plane shear creep modulus are then justified.
- A further reduction in the elastic in-plane shear modulus of lamina G/V under sudden load P_0 is observed. It is demonstrated by comparing the values of modulus G_{12} in the in-plane shear creep test (G_{12} (0.1) = 2926 MPa) and in the in-plane shear test at v_x = 2000 mm/min (G_{12} = 3502 MPa).

In engineering applications, in-plane shear creep and in-plane micro cracks of a polymeric matrix require blocking. This protection can be achieved by forming triangular cells in the in-plane projection of a laminate. A fabric sequence meeting this condition, recommended in engineering applications, is as follows: [B / $[G/B]_n$], where $n \geq 4$, and code B is assigned to a fabric similar to fabric G, but with [0/90] warp/weft directions. Treating the warp and weft of each fabric separately as two laminae, the recommended ply sequence is therefore as follows: [0 / 90 / 45 / –45 / 0 / 90 / 45 / –45 /…/ 0 / 90].

CONCLUSIONS

The final conclusions based on the conducted tests are as follows:

- The strain ratio impact on the course of shear stress--shear strain curves in the quasi-static in-plane shear test of the glass/vinyl-ester lamina reinforced with a balanced orthogonal stitched fabric is significant.
- The identification of in-plane shear strength R_{12} according to the specifications in standards [3, 4] is significantly underestimated.
- The crosshead displacement rate of 2000 mm/min leads to G_{12}, R_{12} parameters authoritative in the design of GFRP laminates with a thermoset matrix.
- For GFRP laminates with a thermoset matrix and ply sequence [0/90/45/–45/0/90/45/–45/…/0/90] the elastic linear model of a lamina should be adequate. This sequence blocks shear creep and micro cracks of the matrix.
- For GFRP laminates with a thermoset matrix at low levels of shear strain and unblocked in-plane shear creep, matrix creep must be taken into consideration in modelling such materials. A linear viscoelastic model for the laminae seems to be adequate in such conditions.

Acknowledgments

This work was supported by the Institute of Mechanics and Computational Engineering, Faculty of Mechanical Engineering, Military University of Technology, Warsaw, Poland [Block Grant No. PBS/23-894/2019]. This support is gratefully acknowledged.

REFERENCES

[1] ASTM D4255/D4255M-01. Standard Test Method for In-Plane Shear Properties of Polymer Matrix Composite Materials by the Rail Shear Method.

[2] ASTM D5379/D5379M-98. Standard Test Method for Shear Properties of Composite Materials by the V-Notched Beam Method.

[3] ASTM D3518/D3518M-94(2001). Standard test method for in-plane shear response of polymer matrix composite materials by tensile test of a ±45° laminate.

[4] EN ISO 14129:1997. Fibre-reinforced plastic composites - Determination of the in-plane shear stress/shear strain response, including the in-plane shear modulus and strength, by the ±45° tension test method.

[5] Zhou G., Davies G.A.O., Characterization of thick glass woven roving/polyester laminates: 1. Tension, compression and shear, Composites 1995, 26(8), 579-586.

[6] Dickson T., Munro M., Selection of an in-plane shear test method based on the shear sensitivity of laminate tensile modulus, Composites 1995, 26(1), 17-24.

[7] Herakovich C.T., Schroedter R.D., Gasser A., Guitard L., Damage evolution in [±45]s laminates with fiber rotation, Composites Science and Technology 2000, 60, 2781-2789.

[8] Van Paepegem W., De Baere I., Degrieck J., Modelling the nonlinear shear stress-strain response of glass fibre-reinforced composites. Part I: Experimental results, Composites Science and Technology 2006, 66, 1455-1464.

[9] Van Paepegem W., De Baere I., Degrieck J., Modelling the nonlinear shear stress–strain response of glass fibre-reinforced composites. Part II: Model development and finite element simulations, Composites Science and Technology 2006, 66, 1465-1478.

[10] Ng W.H., Salvi A.G., Waas A.M., Characterization of the in-situ non-linear shear response of laminated fiber-reinforced composites, Composites Science and Technology 2010, 70, 1126-1134.

[11] Liang Y., Wang H., Gu X., In-plane shear response of unidirectional fiber reinforced and fabric reinforced carbon/epoxy composites, Polymer Testing 2013, 32, 594-601.

[12] Cui H., Thomson D., Pellegrino A., Wiegand J., Petrinic N., Effect of strain rate and fibre rotation on the in-plane shear response of ±45° laminates in tension and compression tests, Composites Science and Technology 2016, 135, 106-115.

[13] Klasztorny M., Nycz D.B., Romanowski R.K., Gotowicki P., Kiczko A., Rudnik D., Effects of operating temperature and accelerated environmental ageing on glass-vinylester composite mechanical properties, Mechanics of Composite Materials 2017, 53(3), 335-350.

[14] Wilczynski A., Klasztorny M., Determination of complex compliances of fibrous polymeric composites, Journal of Composite Materials 2000, 34(1), 2-26.

[15] Klasztorny M., Wilczynski A., Constitutive equations of viscoelasticity and estimation of viscoelastic parameters of unidirectional fibrous polymeric composites, Journal of Composite Materials 2000, 34(19), 1624-1639.

[16] Klasztorny M., Constitutive modelling of resins in compliance domain, Mechanics of Composite Materials 2004, 40(4), 349-358.

[17] Klasztorny M., Constitutive modelling of resins in stiffness domain, Mechanics of Composite Materials 2004, 40(5), 443-452.

[18] Spathis G., Kontou E., Creep failure time prediction of polymers and polymer composites, Composites Science and Technology 2012, 72, 959-964.

[19] Polimal VE-11M Resin. Technical Information, CIECH Sarzyna, Nowa Sarzyna, Poland 2017.

[20] Jones R.M., Mechanics of Composite Materials, 2nd edn, Taylor & Francis, London 1999.

[21] Klasztorny M., Strength of Materials, DWE Press, Wroclaw 2014 (in Polish).

